$Z \to b\bar{b}$ in $U(1)_R$ symmetric supersymmetry

Elizabeth H. Simmons* and Yumian Su†
Department of Physics, Boston University, 590 Commonwealth Ave., Boston, Massachusetts 02215
(Received 16 February 1996)

We compute the one-loop corrections to the $Z \to b\bar{b}$ vertex in the $U(1)_R$ symmetric minimal supersymmetric extension of the standard model. We find that the predicted value of R_b is consistent with the experimental value if the mass of the lighter top squark is no more than 180 GeV. Furthermore, other data combine to place a lower bound of 88 GeV on the mass of the light top squark. A top squark in this mass range should be accessible to searches by experiments at Fermilab and at CERN LEP. [S0556-2821(96)01715-8]

PACS number(s): 12.60.Jv, 13.38.Dg, 14.80.Ly

I. INTRODUCTION

This paper explores the phenomenology of the standard model's minimal supersymmetric [1] extension with a continuous $U(1)_R$ symmetry (hereafter called the ''MR model'') [2]. This model of low-energy supersymmetry has a much smaller-dimensional parameter space than the minimal supersymmetric model (MSSM [3]) with a discrete R parity. As a result, it has two attractive features. First, the MR model makes specific predictions of the values of a number of observables, such as the gaugino masses. In addition, the MR model is free of the superpotential term $\mu H_1 H_2$ and the soft supersymmetry-breaking terms $A\phi^3$ that cause well-known theoretical difficulties in the MSSM.

We focus, in particular, on the recent measurements of R_b,

$$R_b = \frac{\Gamma(Z \to b\bar{b})}{\Gamma(Z \to \text{hadrons})} \tag{1}$$

which yield a value $(R_b)_{\text{expt}} = 0.2205 \pm 0.0016$ [4] that differs markedly from the one-loop standard model prediction $(R_b)_{\text{SM}} = 0.2158$ ($m_t = 174$ GeV) [5]. The oblique and QCD corrections to the b quark and hadronic decay widths of the Z each largely cancel when the ratio is formed, making R_b very sensitive to direct corrections to the Zbb vertex, especially those involving the heavy top quark.

Our work complements some recent papers on SUSY models with discrete R parity. The implications of the R_b measurement for the MSSM are discussed in Refs. [6–8]. A region of the MSSM parameter space that has some phenomenology similar to that of the MR model is studied in [9].

The following section describes the MR model in more detail. We then compute the vertex corrections to R_b in the MR model and find that the result is within 2σ of the experimental value so long as the lighter top squark is light enough (and the charged Higgs boson is heavy enough). Section IV discusses additional constraints that place a lower bound on the mass of the lighter top squark. The information that future experiments may yield is studied in Sec. V; ongoing and upcoming experiments at Fermilab and at the CERN e^+e^- collider CERN LEP should be capable of confirming or excluding the MR model. The last section briefly summarizes our findings.

II. MINIMAL $U(1)_R$ SYMMETRIC SUPERSYMMETRY

The model explored in this paper is the minimal supersymmetric extension of the standard model in which R parity is extended to a continuous U(1) symmetry. The continuous R symmetry is defined by assigning R charges $+1$ to the superspace coordinate θ, $+1$ to matter superfields and 0 to Higgs boson superfields. In terms of component fields, all ordinary particles carry zero R charge while their superpartners have nonzero R charge. The most general $U(1)_R$-symmetric Lagrangian is described by the superpotential

$$W = U^c \lambda_U Q H_2 + D^c \lambda_D Q H_1 + E^c \lambda_E L H_1, \tag{2}$$

where each term has $R = 2$, and the quark and lepton superfields Q, U^c, D^c, L, E^c have the usual SU(3) $\times$ SU(2) $\times$ U(1) gauge interactions. Note the absence of a $\mu H_1 H_2$ term which would violate the $U(1)_R$ symmetry. The most general[1] soft supersymmetry-breaking potential consistent with our symmetries and a Glashow-Iliopoulos-Maiani-(GIM-)like mechanism to naturally suppress flavor-changing neutral currents is

*Electronic address: simmons@bu.edu
†Electronic address: yumian@buphy.bu.edu

[1]Since the $U(1)_R$ symmetry forbids Majorana gaugino masses, the model contains an additional color octet chiral superfield to give a Dirac mass to the gluino. This field appears only in the soft supersymmetry-breaking potential. The gluino mass is relevant to this work in that it renders the one-loop correction to R_b from diagrams with internal gluinos and bottom squarks negligible compared to the effects of the diagrams considered here. We will, therefore, not mention the color octet superfield further. The effects of allowing the gluino to be extremely light in a $U(1)_R$-symmetric model will be considered in future work.

$$\mathcal{L}_{\text{soft}} = m_{H_1}^2 H_1^* H_1 + m_{H_2}^2 H_2^* H_2 + m_Q^2 \tilde{Q}^* \tilde{Q} + m_{U^c}^2 \tilde{U}^{c*} \tilde{U}^c + m_{D^c}^2 \tilde{D}^{c*} \tilde{D}^c + m_L^2 \tilde{L}^* \tilde{L} + m_{E^c}^2 \tilde{E}^{c*} \tilde{E}^c + B H_1 H_2 + \cdots, \tag{3}$$

where we neglect small Yukawa-suppressed corrections to the superpartners' masses. Note the characteristic absence of gaugino mass terms ($M = M' = 0$) and trilinear scalar terms ($A = 0$). For a more detailed description of the model we refer the reader to [2].

The nonstandard one-loop corrections to R_b considered in this paper are of two kinds. One involves the charged-Higgs-boson–top-quark–bottom-quark vertex; the other, the chargino–top-squark–bottom-quark vertex. They, therefore, involve the following parameters: charged Higgs boson mass M_{H^+}, chargino masses $M_{\chi_i^\pm}$, top squark mass eigenvalues $m_{\tilde{t}_{1,2}}$, top squark mixing angle θ, and ratio of Higgs boson vacuum expectation values $\tan\beta$. In the remainder of this section, we focus on those aspects of the model that are directly relevant to determining the above parameters.

First, we should discuss masses. The charged Higgs boson mass is given in terms of the A^0 mass as

$$M_{H^\pm}{}^2 = M_{A^0}{}^2 + M_W{}^2, \tag{4}$$

which implies that $H^\pm$ is heavier than W. The charginos' masses are

$$M_{\tilde{\chi}_1^\pm} = \sqrt{2} M_W \sin\beta, \tag{5}$$

$$M_{\tilde{\chi}_2^\pm} = \sqrt{2} M_W \cos\beta. \tag{6}$$

We will soon find that in this model the charginos are nearly degenerate with the W bosons. As it is relevant to the limits we will ultimately set on the top squark masses, we also note that at the one-loop level, the light neutral Higgs boson has a mass of[2]

$$2M_{h^0}^2 = M_Z^2 + M_A^2 + 2\epsilon - \sqrt{(M_Z^2 + M_A^2)^2 + 4\epsilon^2}, \tag{7}$$

$$\epsilon = \frac{3g^2}{16\pi^2 M_W^2} m_t^4 \ln\left(\frac{m_{\tilde{t}_L}^2 m_{\tilde{t}_R}^2}{m_t^4} \right)$$

in the limit that $\tan\beta \to 1$, which allows bottom squark contributions to be neglected; the reason this limit is preferred will become clear shortly.

The values of the top squark masses are intimately connected to the physics of the lightest superpartner (the photino). The photino is massless at tree level but, together with its Dirac partner $\tilde{H}_\gamma$ (or $\tilde{H}_S$ in the notation of [9]), acquires a Dirac mass at one loop that is generated by the exchange of left- and right-handed top squarks [2]

$$m_{\tilde{\gamma}} = 1.3 \text{ GeV } \cot\beta \left(\frac{m_t}{175\text{GeV}} \right)^2 \times \left| \frac{m_{\tilde{t}_L}{}^2}{m_{\tilde{t}_L}{}^2 - m_t{}^2} \ln\frac{m_{\tilde{t}_L}{}^2}{m_t{}^2} - \frac{m_{\tilde{t}_R}{}^2}{m_{\tilde{t}_R}{}^2 - m_t{}^2} \ln\frac{m_{\tilde{t}_R}{}^2}{m_t{}^2} \right|. \tag{8}$$

From the cosmological point of view, the present mass density is bounded from above by $\Omega_{\tilde{\gamma}} h^2 \leqslant 1$. This implies a lower bound on the cross section for photino annihilation $\sigma_{\tilde{\gamma}}$. Since $\sigma_{\tilde{\gamma}}$ grows as the square of the photino mass, the result is a Lee-Weinberg [10] type of lower bound on the photino mass

$$m_{\tilde{\gamma}}^2 \geqslant \left[\left(\frac{\cos\beta}{1.8 \text{ GeV}} \right)^2 + \frac{1}{(6 \text{ GeV})^2} \sum_{i=1} q_i^4 \left(\frac{M_W}{m_i} \right)^4 \right]^{-1} \times (\Omega_{\tilde{\gamma}} h^2)^{-1}, \tag{9}$$

where i runs over all squarks and sleptons of charge q_i and mass m_i such that the corresponding quarks and leptons are the possible final states of photino annihilation [2].

Since the photino cannot be massless, Eq. (8) implies that the top squarks $\tilde{t}_L$ and $\tilde{t}_R$ cannot be degenerate in the MR model. If one supposes $\tilde{t}_R$ to be lighter than $\tilde{t}_L$, then, for a given mass of $\tilde{t}_R$, one will find a lower bound on the mass of $\tilde{t}_L$. For example, if $m_{\tilde{t}_R} = 80(100)$ GeV, then $m_{\tilde{t}_L} \geqslant 280(400)$ GeV. The top squark mass eigenstates $\tilde{t}_1$ and $\tilde{t}_2$ are related to $\tilde{t}_R$ and $\tilde{t}_L$ by

$$\tilde{t}_1 = \tilde{t}_R \cos\theta + \tilde{t}_L \sin\theta, \quad \tilde{t}_2 = -\tilde{t}_R \sin\theta + \tilde{t}_L \cos\theta, \tag{10}$$

which define the mixing angle θ. We find that in order for the top squark mass eigenvalues $m_{\tilde{t}_1}$, $m_{\tilde{t}_2}$ to be real, the top squark mixing angle θ must be less than ten degrees. Thus, in the MR model, $\tilde{t}_1 \approx \tilde{t}_R$.

Finally, we need to discuss $\tan\beta$. We have already seen that the overall scale of $m_{\tilde{\gamma}}$ is of the order of 1 GeV. This makes the decay $Z \to \tilde{H}_\gamma \tilde{H}_\gamma$ possible, which in turn makes the Z invisible width larger than it is in the standard model. The branching fraction of $Z \to \tilde{H}_\gamma \tilde{H}_\gamma$ is suppressed by a factor of $\cos^2 2\beta$ relative to the standard model branching fraction for one ν species, $Z \to \nu_l \bar{\nu}_l$. Thus, we have

$$\frac{\Gamma(Z \to \text{invisible})}{\Gamma(Z \to \nu\bar{\nu})} = 3 + \cos^2 2\beta. \tag{11}$$

[2]In the MSSM, there are also contributions involving the coefficient μ of the $H_1 H_2$ term in the superpotential and the coefficient A of the trilinear scalar operators in the supersymmetry-breaking terms. Those two coefficients vanish in the MR model because of the continuous U(1)$_R$ symmetry.

[3]Since our purpose is determine whether the MR model is phenomenologically viable at the weak scale without regard to its high-energy origins, we shall not impose the further constraint $\tan\beta > 1$ which naturally appears in grand-unified-theory- (GUT-)inspired models with radiative electroweak symmetry breaking.

The experimental limit on the number of light neutrino species [11], $N_\nu = 2.983 \pm 0.025$, therefore, implies that at 95% C.L. $\tan\beta$ lies very close[3] to unity:

$$0.88 < \tan\beta < 1.14. \quad (12)$$

The several parameters of the MR model are now essentially reduced to two. The stringent constraint $\tan\beta \approx 1$ forces the charginos to be approximately degenerate with the W. The requirement that the photino not be massless forces the top squark mixing angle to be less than 10°; we take $\theta = 0°$ throughout our calculations. When $\theta = 0°$, the superpartner of the right-handed top quark, $\tilde{t}_R$ is identical to the light top squark mass eigenstate $\tilde{t}_1$; since only $\tilde{t}_R$ enters the loop affecting the Z coupling to left-handed b quarks, R_b depends on $m_{\tilde{t}_1}$ but not on $m_{\tilde{t}_2}$. We are left with only two parameters on which R_b will depend: M_{H^+} and $m_{\tilde{t}_1}$.

III. $Z \to b\bar{b}$ IN THE MR MODEL

In order to test the MR model, we can separate contributions to R_b into those occurring in both the standard and MR models and those additional effects present only in the MR model. In the notation of Refs. [12,6],

$$R_b = R_b^{\rm SM}(m_t) + R_b^{\rm SM}(0)[1 - R_b^{\rm SM}(0)][\nabla_b^{\rm MR}], \quad (13)$$

$$\nabla_b^{\rm MR} \equiv \nabla_b{}^{\rm MR}(m_t) - \nabla_b{}^{\rm MR}(0),$$

where $R_b^{\rm SM}(m_t = 174\ {\rm GeV}) = 0.2158$ is the one-loop level standard model prediction using a top quark mass of $m_t = 174$ GeV, $R_b^{\rm SM}(0) = 0.220$ is the standard model prediction assuming a massless top quark [7], and $\nabla_b{}^{\rm MR}(m_t)$ is the sum of the one-loop interference with the tree graph divided by the squared amplitude of the tree graph. In the MR model, there are two relevant types of nonstandard one-loop vertex diagrams: those with internal charged Higgs bosons and top quarks, and those with internal charginos and top squarks. Their contributions to $\nabla_b{}^{\rm MR}(m_t)$ are proportional to $(m_t/\sqrt{2}M_W\tan\beta)^2$; the details of the calculation are presented in the Appendix. Another type of vertex diagram with internal neutralinos and bottom squarks makes contributions proportional to $(\sqrt{2}m_b\tan\beta/M_W)^2$, which is negligible in the MR model because $\tan\beta \approx 1$; we omit these.

In Fig. 1, we plot $\nabla_b{}^{H^+}$, the contribution from the $H^+ - t$ vertex diagrams to $\nabla_b^{\rm MR}$, as a function of $M_{H^\pm}$, when $\tan\beta$ is taken to be 1, 0.9, or 1.1. The overall sign is negative and the value of $\nabla_b^{H^+}$ shifts by 20% as $\tan\beta$ varies from 1 to 1.1 or to 0.9. Figure 2 shows the corresponding contribution from $\chi - \tilde{t}$ loops to $\nabla_b^{\chi^+}$, as a function of the light top squark mass $m_{\tilde{t}_1}$ when the mixing angle θ between top squarks is 0° ($m_{\tilde{t}_1} = m_{\tilde{t}_R}$). The result is positive, and the deviation due to a 10% shift in $\tan\beta$ is negligible.

Thus, the net shift in R_b is due to a balance between the oppositely signed contributions from the two types of loop diagrams. In Fig. 3, we set $m_{\tilde{t}_1} = 100$ GeV and plot R_b as a function of M_{H^+} for a range of $\tan\beta$; we can clearly infer a lower bound on the allowed value of M_{H^+} at fixed $m_{\tilde{t}_1}$. Likewise, Fig. 4 shows the dependence of R_b on $m_{\tilde{t}_1}$ for

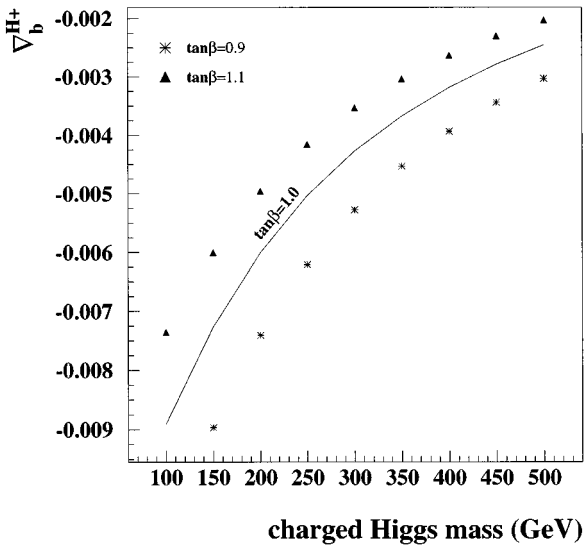

FIG. 1. $\nabla_b^{H^+}$ as a function of M_{H^+} for $m_t = 174$ GeV and three values of $\tan\beta$.

$M_{H^+} = 500$ GeV; we can infer an upper bound on $m_{\tilde{t}_1}$ for fixed M_{H^+}. In subsequent diagrams we plot results only for $\tan\beta = 1$ and keep in mind that an increase of 10% in $\tan\beta$ corresponds to an increase of about 0.1% in R_b for given M_{H^+} and $m_{\tilde{t}_1}$.

Figure 5 shows how the experimental 95% C.L. lower bound on R_b separates the M_{H^+} vs $m_{\tilde{t}_1}$ parameter space into allowed and disallowed regions. Recall that the $H^+ - t$ loop gives negative corrections to R_b, while the $\chi^+ - \tilde{t}$ loop gives positive corrections. Since the standard model prediction for R_b lies well below the experimental lower bound, some positive contribution is required to bring the MR prediction for R_b into agreement with the experimental value. Hence, by taking the charged Higgs boson mass to infinity, one finds an

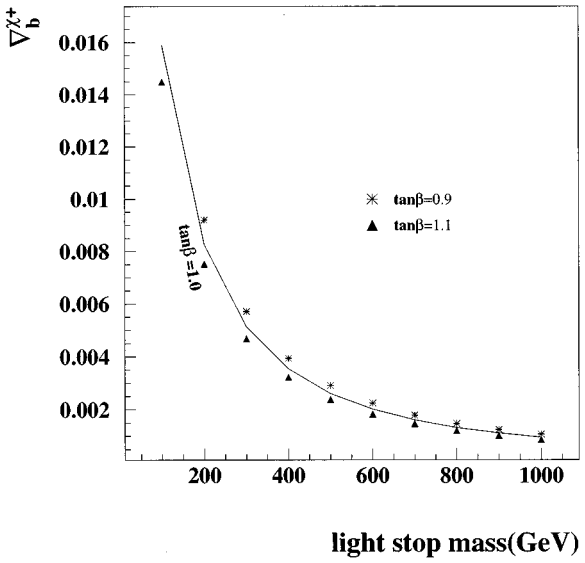

FIG. 2. $\nabla_b^{\chi^+}$ as a function of $m_{\tilde{t}_1}$ for $m_t = 174$ GeV, $\theta = 0°$, and three values of $\tan\beta$.

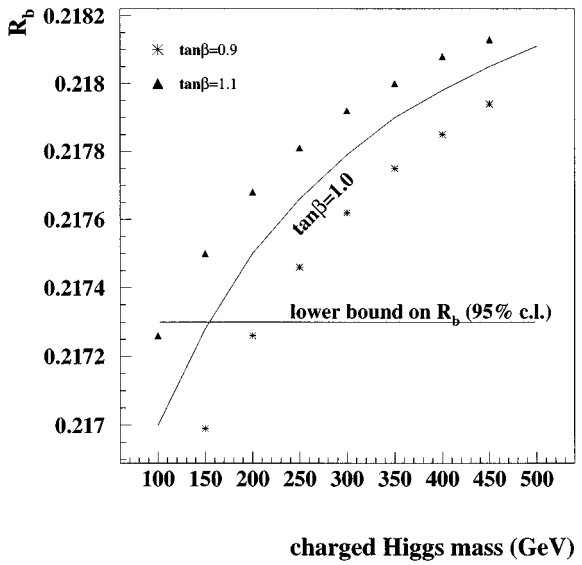

FIG. 3. R_b as a function of M_{H^+} for $m_{\tilde{t}_1}=100$ GeV.

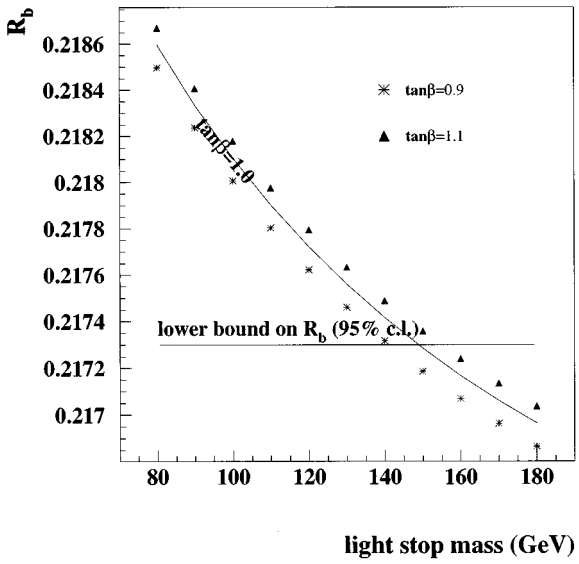

FIG. 4. R_b as a function of $m_{\tilde{t}_1}$ for $M_{H^+}=500$ GeV.

asymptotic upper limit on the light top squark mass of 180 GeV at 95% C.L. The precise upper bound on $m_{\tilde{t}_1}$ will be smaller than 180 GeV for any finite M_{H^+}, due to the negative contribution to R_b from the H^+-t loop. For any fixed M_{H^+}, the corresponding upper bound on $m_{\tilde{t}_1}$ can be read from Fig. 5.

IV. CONSTRAINTS FROM OTHER EXTANT DATA

Combining the information gleaned from R_b with other experimental data yields additional constraints on the MR model.

First, we can use the lower bounds on the mass of the light neutral Higgs boson (h_0) to set a limit on $m_{\tilde{t}_2}$. Recall that the h_0 mass depends on the product of the top squark masses at the one-loop level. Thus, for a given light top squark mass, the heavier the heavy top squark, the heavier the neutral Higgs boson. Then, by setting the light top squark's mass to the maximum value of 180 GeV and using the lower bound[4] of 56 GeV that ALEPH [13] sets on the h_0 mass in the MR model, we find that $m_{\tilde{t}_2} \geq 0.7$ TeV. If the mass of the $\tilde{t}_1$ is less than 180 GeV, the lower bound on $m_{\tilde{t}_2}$ increases accordingly.

The information on the masses of the top squarks provides limits on the photino mass, which depends on the masses of both top squarks at the one-loop level. To maintain naturalness, the masses of the sparticles should be of the order of a TeV. If the mass of the heavy top squark lies between 0.7 and 10 TeV, the photino mass is between 2.5 and 10 GeV.

This is very helpful because both D0 [14] and the LEP Collaborations have set limits on the allowed region of the $m_{\tilde{\gamma}}$ vs $m_{\tilde{t}_1}$ plane. For the narrow range of photino masses allowed in the MR model, these experiments essentially constrain the light top squark mass to take values only in the ranges (0–12 GeV), (44 GeV–46 GeV), and (88 GeV–180 GeV). This is shown in Fig. 6.

A closer look then excludes the case $0 \leq m_{\tilde{t}_1} \leq 12$ GeV. If the $\tilde{t}_1$ is this light, then in order for the h_0 mass to exceed the LEP lower bound of 56 GeV, the heavy top squark would have to be heavier than about 24 TeV. As a result, the top

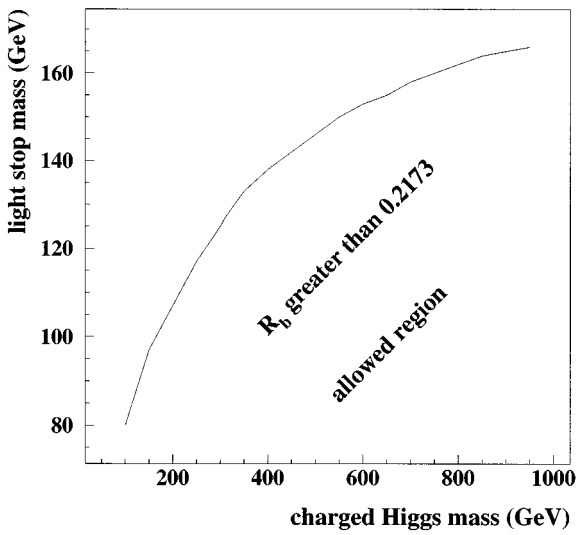

FIG. 5. R_b sets constraints on the model's parameter space. The lower right region is allowed, while the upper left region is excluded, at 95% C.L. For a given charged Higgs boson mass, there is an upper limit on the mass of the light top squark.

[4]The limit lies between those on the standard model Higgs boson and on the MSSM Higgs boson because the strength of the ZZ^*h coupling lies between the extremes of the other two models. The ZZ^*h coupling is proportional to $\sin(\beta-\alpha)$ where α is the mixing angle that diagonalizes the neutral Higgs boson mass matrix. Throughout the parameter space of the MR model, $\sin^2(\beta-\alpha)$ is greater than about 0.75; it can take on smaller values in the MSSM and is 1.0 in the standard model.

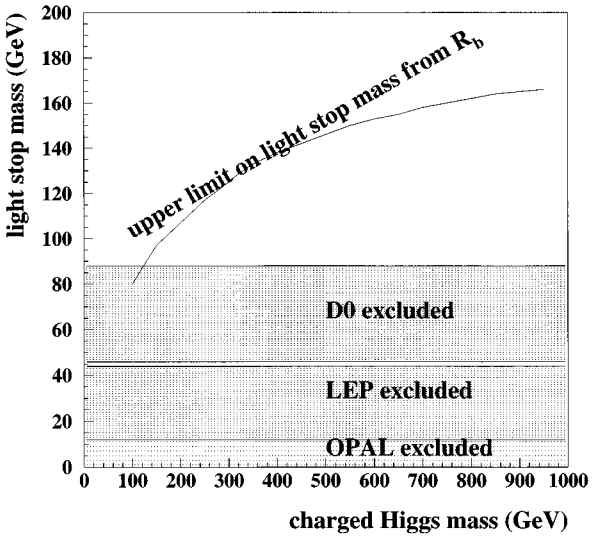

FIG. 6. The upper limit on the light top squark mass deduced from R_b (see Fig. 5) is compared with D0 and LEP results. Preliminary L3 data also excludes the window around $m_{\tilde{t}_1}=45$ GeV.

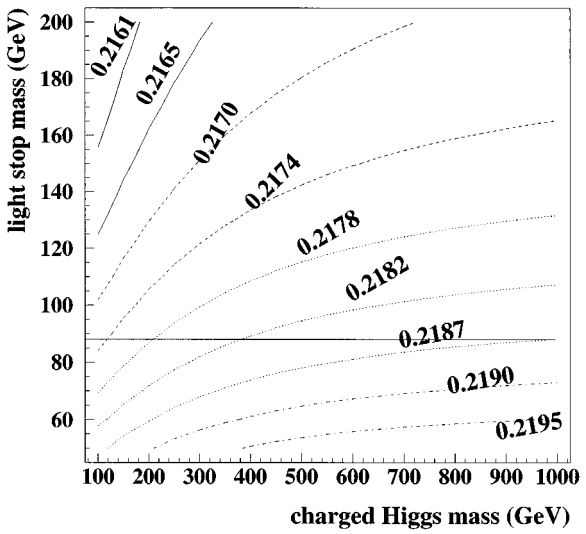

FIG. 7. Contours of constant R_b in the $(M_{H^+}, m_{\tilde{t}_1})$ plane. The size of the MR model's allowed parameter space and the upper limit on $m_{\tilde{t}_1}$ are quite sensitive to the value of the lower bound on R_b. The lower limit $m_{\tilde{t}_1}\geqslant 88$ GeV derived from D0 and LEP data is shown for comparison.

squark mixing angle would be almost precisely zero. The combination of such a light $\tilde{t}_1$ and such a small mixing angle has already been ruled out by OPAL [15]. The mass of the $\tilde{t}_1$ in the MR model must, therefore, lie in one of the upper two allowed ranges.

In fact, preliminary results from the L3 Collaboration based on the recent LEP run at a center-of-mass energy of 130–140 GeV show no sign of a top squark in the mass range below about 50 GeV [16]. It is, therefore, likely that the middle mass range for $\tilde{t}_1$ in the MR model is also excluded.

V. FUTURE EXPERIMENTAL INPUT

We now briefly discuss several measurements that may provide useful information on the MR model in the future. These run the gamut from precision measurements to searches for new particles.

A. $b\to s\gamma$

Since a light top squark could have an appreciable effect on the branching ratio for $b\to s\gamma$, we compare the ratio measured at CLEO with that predicted by the MR model. The branching ratio of $b\to s\gamma$ measured in CLEO [17] is

$$B(b\to s\gamma)=(2.32\pm 0.57\pm 0.35)\times 10^{-4}.$$

The MR model predicts a branching ratio within 2σ of the CLEO result whenever the light top squark weighs in the regions of (44 GeV–46 GeV) and (88 GeV–180 GeV). Until future experiments reduce the errors on the $b\to s\gamma$ branching ratio, this particular quantity will not help constrain the MR model.

B. $t\to Wb$

The relatively light mass of the $\tilde{t}_1$ in the MR model makes it possible for the top quark to decay to a top squark and a neutralino. As a result, the branching ratio for the standard top quark decay mode $B(t\to Wb)$, which is approximately 100% in the standard model, would be only 70–80% in the MR model. The limits on this branching ratio from Collider Detector at Fermilab (CDF) data [18] are not strong enough to constrain the MR model, yet.

C. R_b

Once all of the 1994–1995 data from LEP are analyzed, the precise experimental limits on R_b may shift. The potential consequences for the MR model are quite interesting.

Figure 7 shows contours corresponding to several values of R_b near the current experimental 2σ lower bound. These curves imply that while the value of R_b in the MR model is consistent with the present experimental value of R_b, the theoretical prediction generally lies well below the experimental central value of 0.2205 [4].

As a result, the size of the allowed parameter space of the MR model depends sensitively on the experimental determination of R_b. Clearly, even a very small downward shift in the central value of R_b would allow $m_{\tilde{t}_1}$ to be heavier than 180 GeV. On the other hand, an upward shift in the central value or an improvement in the errors on the current central value of R_b could reduce the upper bound on $m_{\tilde{t}_1}$ to a value below 88 GeV, i.e., into the region already excluded by D0 and LEP.

D. Searches for light top squarks and h^0

Searches for top squarks in the D0 and CDF experiments should explore the remaining parameter space of the MR model. For example, the mass range $m_{\tilde{t}_1}\geqslant 88$ GeV can be probed by seeking top squarks in the decay channels $\tilde{t}\to\chi^{\pm}b$, in addition to the $\tilde{t}\to c\tilde{\gamma}$ channel already explored by D0. The upcoming experiments at LEP II will also be sensitive to part of the allowed mass range for light top squarks.

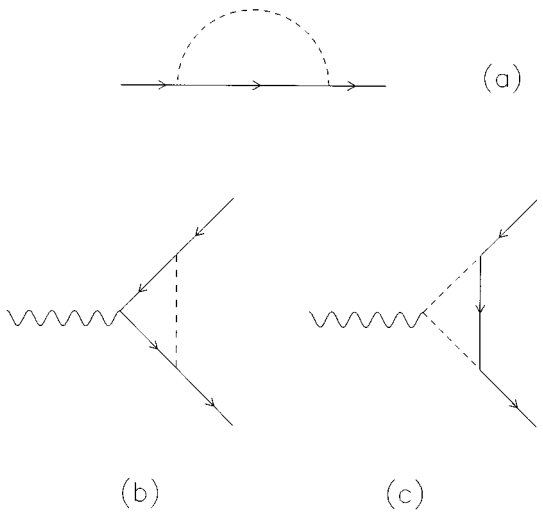

FIG. 8. One-loop Feynman diagrams contributing to the renormalization of the $Zb\bar{b}$ vertex. The external gauge boson is a Z^0; the external fermions are b quarks. The internal [fermion, scalar] is either $[t, H^+]$ or $[\chi^+, \tilde{t}]$. The labels (a), (b), (c) on the diagrams correspond to the superscripts on the functions $F_{L,R}$ discussed in the Appendix.

In addition, combining our upper bound on $m_{\tilde{t}_1}$ and the ''naturalness'' upper bound on $m_{\tilde{t}_2}$ with Eq. (7) implies an upper bound of $\sim$ 90 GeV on M_{h_0}. Searches for h^0 are discussed in Ref. [2].

VI. CONCLUSION

By considering the value of R_b predicted by minimal U(1)$_R$-symmetric supersymmetry, we have shown that this model is consistent with experiment so long as the light top squark weighs no more than 180 GeV. Other considerations, including top squark searches at LEP and D0, further restrict the top squark mass to satisfy $m_{\tilde{t}_1} \geqslant 88$ GeV. The light top squark of the MR model should, therefore, be accessible to D0, CDF, and the LEP II experiments.

ACKNOWLEDGMENTS

We thank G. Bonini, D. Brown, J. Butler, R. S. Chivukula, I. DasGupta, B. Dobrescu, D. Finnell, and B. Zhou for useful discussions and comments on the manuscript. E.H.S. acknowledges the support of the NSF Faculty Early Career Development (CAREER) program and of the DOE Outstanding Junior Investigator program. This work was supported in part by the National Science Foundation under Grant No. PHY-9501249, and by the Department of Energy under Grant No. DE-FG02-91ER40676.

APPENDIX

This appendix contains more detail on the calculation of the shift in R_b. We take the explicit formulas from Ref. [12]. For the reader's convenience, we list the formulas below; note that we set m_b to zero in our calculations since $\tan\beta = 1$ in the MR model. Starting from Eq. (13),

$$R_b = R_b{}^{\rm SM}(m_t) + R_b{}^{\rm SM}(0)[1 - R_b{}^{\rm SM}(0)][\nabla_b^{\rm MR}],$$

$$\nabla_b^{\rm MR} \equiv \nabla_b{}^{\rm MR}(m_t) - \nabla_b{}^{\rm MR}(0),$$

we can separate $\nabla_b^{\rm MR}$ into the pieces contributed by the diagrams with charged Higgs bosons and by those with charginos

$$\nabla_b{}^{\rm MR} = \nabla_b{}^{H^+} + \nabla_b{}^{\chi^+}, \tag{A1}$$

where

$$\nabla_b{}^{H^+} = \nabla_b{}^{H^+}(m_t) - \nabla_b{}^{H^+}(0),$$

$$\nabla_b{}^{\chi^+} = \nabla_b{}^{\chi^+}(m_t) - \nabla_b{}^{\chi^+}(0). \tag{A2}$$

The functions $\nabla_b{}^{H^+}(m)$ and $\nabla_b{}^{\chi^+}(m)$ are each of the form

$$\nabla_b(m) = \frac{\alpha}{4\pi \sin^2\theta_W}\left[\frac{2v_L F_L(M_Z^2, m) + 2v_R F_R(M_Z^2, m)}{v_L^2 + v_R^2}\right], \tag{A3}$$

where

$$v_L = -\tfrac{1}{2} + \tfrac{1}{3}\sin^2\theta_W, \quad v_R = \tfrac{1}{3}\sin^2\theta_W. \tag{A4}$$

Explicit expressions for the functions $F_{L,R}$ are given below; those for diagrams with internal Higgs bosons are first, followed by those for diagrams with internal charginos.

The contributions from diagrams with internal charged Higgs bosons are (see Fig. 8 for the meaning of the superscripts on the $F_{L,R}$)

$$F_{L,R}^{(a)} = b_1(M_{H^+}, m_t, m_b^2)\ v_{L,R}\ \lambda_{L,R}^2,$$

$$F_{L,R}^{(b)} = \left(\left[\frac{M_Z^2}{\mu_R^2} c_6(M_{H^+}, m_t, m_t) - \frac{1}{2} - c_0(M_{H^+}, m_t, m_t)\right] v_{R,L}^{(t)} + \frac{m_t^2}{\mu_R^2} c_2(M_{H^+}, m_t, m_t) v_{L,R}^{(t)}\right)\lambda_{L,R}^2,$$

$$F_{L,R}^{(c)} = c_0(m_t, M_{H^+}, M_{H^+})(\tfrac{1}{2} - \sin^2\theta_W)\lambda_{L,R}^2, \tag{A5}$$

where

$$v_L^{(t)} = \tfrac{1}{2} - \tfrac{2}{3}\sin^2\theta_W, \quad v_R^{(t)} = -\tfrac{2}{3}\sin^2\theta_W, \tag{A6}$$

$$\lambda_L = \frac{m_t}{\sqrt{2} M_W \tan\beta}, \quad \lambda_R = \frac{m_b \tan\beta}{\sqrt{2} M_W},$$

and μ_R is the mass scale which arises in dimensional regularization.

The contributions from the diagrams with internal charginos are

$$F_{L,R}^{(a)} = \sum_{i=1,2}\sum_{j=1,2} b_1(\tilde{m}_j, M_i, m_b^2) v_{L,R} |\Lambda_{ji}^{(L,R)}|^2,$$

$$F_{L,R}^{(c)} = \sum_{i=1,2}\sum_{j=1,2}\sum_{k=1,2} c_0(M_k, \tilde{m}_i, \tilde{m}_j) \times \left(\tfrac{2}{3}\sin^2\theta_W \delta_{ij} - \frac{1}{2} T_{i1}^* T_{j1}\right)\Lambda_{ik}^{L,R}\Lambda_{jk}^{*L,R},$$

$$F_{L,R}^{(b)}=\sum_{i=1,2}\sum_{j=1,2}\sum_{k=1,2}\left(\left[\frac{M_Z^2}{\mu_R^2}c_6(\tilde{m}_k,M_i,M_j)-\tfrac{1}{2}-c_0(\tilde{m}_k,M_i,M_j)\right]O_{ij}^{R,L}+\frac{M_iM_j}{\mu_R^2}c_2(\tilde{m}_k,M_i,M_j)O_{ij}^{L,R}\right)\Lambda_{ki}^{L,R}\Lambda_{kj}^{*L,R},\tag{A7}$$

where

$$\Lambda_{ij}^{L}=T_{i1}V_{j1}^{*}-\left[\frac{m_t}{\sqrt{2}M_W\sin\beta}\right]T_{i2}V_{j2}^{*},$$

$$\Lambda_{ij}^{R}=-\left[\frac{m_b}{\sqrt{2}M_W\cos\beta}\right]T_{i1}U_{j2},\tag{A8}$$

M_i are the chargino masses, $\tilde{m}_i$ are the top squark mass eigenvalues, and

$$O_{ij}^{L}=-\cos^2\theta_W\delta_{ij}+\tfrac{1}{2}U_{i2}^{*}U_{j2},$$

$$O_{ij}^{R}=-\cos^2\theta_W\delta_{ij}+\tfrac{1}{2}V_{i2}^{*}V_{j2},\tag{A9}$$

$$T=\begin{pmatrix}\cos\theta & \sin\theta\\ -\sin\theta & \cos\theta\end{pmatrix},\quad U=\begin{pmatrix}0 & 1\\ 1 & 0\end{pmatrix},\quad V=\begin{pmatrix}1 & 0\\ 0 & 1\end{pmatrix}.\tag{A10}$$

Note that in the limit where $\tan\beta=1$, the matrices U and V need only satisfy $(U^*)^{-1}V=\left(\begin{smallmatrix}0 & 1\\ 1 & 0\end{smallmatrix}\right)$; for instance, the pair

$$U=\frac{1}{\sqrt{2}}\begin{pmatrix}1 & 1\\ -1 & 1\end{pmatrix},\quad V=\frac{1}{\sqrt{2}}\begin{pmatrix}1 & 1\\ 1 & -1\end{pmatrix}\tag{A11}$$

are also appropriate.

Throughout the preceding account, the b's and c's are reduced Passarino-Veltman functions [19],

$$[b_0,b_1,b_2,b_3](m_1,m_2,q^2)=\int_0^1 dx\ln[-q^2x(1-x)+xm_1^2+(1-x)m_2^2-i\epsilon]\ /\mu_R^2\times[-1,\ x,(1-x),x(1-x)],$$

$$[c_0,c_1](m_1,m_2,m_3)=\int dxdydz\,\delta(x+y+z-1)\ln(\Delta/\mu_R^2)\times[1,\ z],$$

$$[c_2,c_3,c_4,c_5,c_6,c_7](m_1,m_2,m_3)=\int dxdydz\,\delta(x+y+z-1)(\mu_R^2/\Delta)[1,\ z,z^2,z^3,xy,xyz],\tag{A12}$$

where

$$\Delta=zm_1^2+xm_2^2+ym_3^2-z(1-z)m_b^2-xyM_Z^2-i\epsilon\tag{A13}$$

and we have corrected small typos in the definitions of b_0, c_6, and c_7 as quoted in Ref. [12].

[1] P. Fayet, Nucl. Phys. **B90**, 104 (1975); Phys. Lett. **69B**, 489 (1977); G. R. Farrar and P. Fayet, *ibid.* **76B**, 575 (1978); E. Witten, Nucl. Phys. **B188**, 513 (1981); S. Dimopoulos and H. Georgi, *ibid.* **B193**, 150 (1981); N. Sakai, Z. Phys. C **11**, 153 (1981); L. Ibañez and G. Ross, Phys. Lett. **105B**, 439 (1981); R. K. Kaul, *ibid.* **109B**, 19 (1982); M. Dine, W. Fischler, and M. Srednicki, Nucl. Phys. **B189**, 575 (1981); S. Dimopoulos and S. Raby, *ibid.* **B192**, 353 (1981).

[2] L. J. Hall and L. Randall, Nucl. Phys. **B352**, 289 (1991); L. Randall and N. Rius, Phys. Lett. B **286**, 299 (1992); N. Rius and E. H. Simmons, Nucl. Phys. **B416**, 722 (1994).

[3] See, e.g., the following reviews: H. P. Nilles, Phys. Rep **110**, 1 (1984); H. E. Haber and G. L. Kane, *ibid.* **117**, 75 (1985); J. F. Gunion and H. E. Haber, Nucl. Phys. **B272**, 1 (1986), **B402**, 567(E) (1993).

[4] P. B. Renton, Rapporteur talk at the International Conference on High Energy Physics, Beijing, 1995 (unpublished); LEP Electroweak Working Group Report No. LEPEWWG/95-02, 1995 (unpublished).

[5] P. Langacker, Report No. hep-ph/9408310 (unpublished); P. Langacker and J. Erler, Phys. Rev. D **50**, 1304 (1994); A. Blondel, Report No. CERN PPE/94-133, http://alephwww.cern.ch/ALEPHGENERAL/reports/reports.html (unpublished).

[6] J. D. Wells, C. Kolda, and G. L. Kane, Phys. Lett. B **338**, 219 (1994).

[7] J. D. Wells and G. L. Kane, Phys. Rev. Lett. **76**, 869 (1996).

[8] X. Wang, J. L. Lopez, and D. V. Nanopoulos, Phys. Rev. D **52**, 4116 (1995); J. Ellis, J. L. Lopez, and D. V. Nanopoulos, ''Supersymmetry and R_b in the light of LEP 1.5,'' Report No. hep-ph/9512288, 1995 (unpublished).

[9] J. L. Feng, N. Polonsky, and S. Thomas, ''The Light Higgsino-Gaugino Window,'' Report No. hep-ph/9511324, 1995 (unpublished).

[10] B. W. Lee and S. Weinberg, Phys. Rev. Lett. **39**, 165 (1977).

[11] Particle Data Group, L. Montanet *et al.*, Phys. Rev. D **50**, 1416 (1994).

[12] M. Boulware and D. Finnell, Phys. Rev. D **44**, 2054 (1991).

[13] ALEPH Collaboration, D. Buskulic *et al.*, Phys. Lett. B **313**, 312 (1993).

[14] D0 Collaboration, S. Abachi *et al.*, Phys. Rev. Lett. **76**, 2222 (1996).

[15] OPAL Collaboration, Phys. Lett. B **337**, 207 (1994).

[16] D. Strickland, ''Summary of L3 Results from The November 1995 LEP Run at 130-140 GeV,'' Talk presented at the LEP Collaboration meeting at CERN, 1995, http://hpl3sn02.cern.ch/conf.html (unpublished).

[17] CLEO Collaboration, Phys. Rev. Lett. **74**, 2885 (1995).

[18] J. Incandela, ''CDF Top Quark Production and Mass,'' Talk presented at the 6th International Symposium on Heavy Flavor Physics, 1995, Pisa, Italy, FERMILAB-CONF-95/237-E, CDF/PUB/TOP/PUBLIC/3273 (unpublished).

[19] C. Ahn, B. Lynn, M. Peskin, and S. Selipsky, Nucl. Phys. **B309**, 221 (1988).